Developmental Biology 370 (2012) 173–186

Contents lists available at SciVerse ScienceDirect

Developmental Biology

journal homepage: www.elsevier.com/locate/developmentalbiology

Pan-epicardial lineage tracing reveals that epicardium derived cells give rise to myofibroblasts and perivascular cells during zebrafish heart regeneration

Juan Manuel González-Rosa, Marina Peralta, Nadia Mercader*

Department of Cardiovascular Development and Repair, Centro Nacional de Investigaciones Cardiovasculares (CNIC), Calle Melchor Fernández Almagro 3, E-28029 Madrid, Spain

ARTICLE INFO

Article history:
Received 4 October 2011
Received in revised form
27 June 2012
Accepted 10 July 2012
Available online 1 August 2012

Keywords:
Zebrafish heart regeneration
Epicardium
Cardiomyocytes
Migration
Fibroblasts
Scar

ABSTRACT

Myocardial infarction (MI) leads to a severe loss of cardiomyocytes, which in mammals are replaced by scar tissue. Epicardial derived cells (EPDCs) have been reported to differentiate into cardiomyocytes during development, and proposed to have cardiomyogenic potential in the adult heart. However, mouse MI models reveal little if any contribution of EPDCs to myocardium. In contrast to adult mammals, teleosts possess a high myocardial regenerative capacity. To test if this advantage relates to the properties of their epicardium, we studied the fate of EPDCs in cryoinjured zebrafish hearts. To avoid the limitations of genetic labelling, which might trace only a subpopulation of EPDCs, we used cell transplantation to track all EPDCs during regeneration. EPDCs migrated to the injured myocardium, where they differentiated into myofibroblasts and perivascular fibroblasts. However, we did not detect any differentiation of EPDCs nor any other non-cardiomyocyte population into cardiomyocytes, even in a context of impaired cardiomyocyte proliferation. Our results support a model in which the epicardium promotes myocardial regeneration by forming a cellular scaffold, and suggests that it might induce cardiomyocyte proliferation and contribute to neoangiogenesis in a paracrine manner.

Introduction

In response to myocardial infarction (MI), the most common cause of heart failure in humans, cardiomyocytes undergo ischemic cell death and are replaced by scar tissue. Finding ways to replenish the lost myocardium is a key research goal, and potential sources of exogenous or resident stem cells are being evaluated for their capacity to differentiate into functional and electrically-coupled cardiomyocytes (Alexander and Bruneau, 2010; Mercola et al., 2011).

The role of the epicardium during myocardial regeneration has attracted growing interest (Vieira and Riley, 2010). In the adult, the epicardium constitutes an epithelial layer enveloping the heart. During development, a subset of epicardial cells undergoes epithelial-to-mesenchymal transition (EMT), invading the subepicardial space to give rise to epicardial derived cells (EPDCs) (reviewed in Carmona et al., 2010; Perez-Pomares and de la Pompa, 2011). The epicardium of the developing heart expresses *Wilm's tumor suppressor gene 1* (*Wt1*), which promotes epicardial EMT (Kreidberg et al., 1993; Martinez-Estrada et al., 2010; Moore et al., 1999; von Gise et al., 2011). In mice, lineage tracing showed that *Wt1*$^+$ cells give rise to smooth muscle cells of the coronary vasculature and to fibroblasts (intracardiac fibroblasts and fibroblasts of the tunica adventitia and the annulus fibrosus). In addition, *Wt1*$^+$ cells were found to contribute 4% of the total number of cardiomyocytes, predominantly populating the intraventricular septum, but also in ventricular wall and atria (Zhou et al., 2008). Similar results were obtained by fate mapping cells expressing T box transcription factor 18 (Cai et al., 2008). However, although *Tbx18* is expressed in epicardial cells, expression has also been reported in the developing myocardium, casting doubt on its usefullness as an epicardial reporter gene (Christoffels et al., 2009). A third gene broadly expressed in the epicardium is *Tcf21* (also known as *Pod1, capsulin, and epicardin*) (Hidai et al., 1998; Lu et al., 1998; Quaggin et al., 1999; Robb et al., 1998). Genetic lineage tracing in mouse and zebrafish showed that *Tcf21*$^+$ cells give rise to intracardiac fibroblasts, but not to coronary smooth muscle or endothelial cells (Acharya et al., 2011; Kikuchi et al., 2011a). These genetic lineage tracing analyses appear to conflict with experimental evidence from chick that EPDCs are the major progenitor source of coronary vascular endothelial cells, but this has recently been resolved by the discovery of scleraxis- and semaphorin3D-expressing EPDCs in the developing mouse heart that give rise to endothelial cells of the coronary vasculature (Katz et al., 2012). The non or incomplete overlap of fate maps found with these lines suggests that none of them labels the entire epicardial cell pool and thus supports the idea that the epicardium is a mixture of cells with

* Corresponding author. Fax: +34 914531204.
E-mail address: nmercader@cnic.es (N. Mercader).

0012-1606/$ - see front matter © 2012 Elsevier Inc. All rights reserved.
http://dx.doi.org/10.1016/j.ydbio.2012.07.007

differing gene expression profiles. In addition, the contribution of EPDCs to the developing myocardium has not been confirmed in the chick or zebrafish (Kikuchi et al., 2011a; Manner, 1999). This discrepancy might reflect inter-species divergence or simply the differing experimental approaches used to study EPDC fate. EPDC fate studies would therefore benefit from the use of a more unbiased lineage-tracing approach.

Several animal models of MI show that the early response to heart injury includes a reactivation of epicardial genes usually expressed only during development, such as *Tbx18* and *Wt1* (Lepilina et al., 2006; Limana et al., 2009). While reactivation of these genes is organ-wide initially, it later becomes restricted to the site of damage, suggesting that signals emanating from the injured area (IA) control epicardial responses. Concomitantly, the epicardium undergoes EMT and proliferates, leading to the formation of a thickened epicardial cap covering the injured myocardium (González-Rosa et al., 2011; Kim et al., 2010; Smart et al., 2010; Zhou et al., 2011a). Unlike the situation during development, in response to injury EPDCs remain on the heart surface and do not invade the myocardium (Zhou et al., 2011a, b). This observation suggests a role for the epicardium during the healing process, supported by the finding that EPDCs secrete proangiogenic factors such as VEGFA and CXCL12 and thus control neoangiogenesis through a paracrine action (Zhou et al., 2011a).

In addition to its trophic function, the epicardium might thus be a source of progenitor cells for the repair of injured cardiac tissue. Cells positive for the stem-cell markers c-kit and CD34 have been detected in the subepicardial space in fetal and adult human hearts (Limana et al., 2007). In culture, these cells can acquire a myocardial, endothelial or smooth muscle phenotype (van Tuyn et al., 2007). Recent lineage-tracing experiments analysing *Wt1*-progeny revealed that upon MI in mice epicardial cells give rise to fibroblasts, myofibroblasts and smooth muscle cells, which accumulate in the thickened epicardial cap. However, $Wt1^+$ cells do not differentiate into endothelial cells or cardiomyocytes (Zhou et al., 2011a).

Unlike adult mammals, the hearts of urodeles and teleosts have a high regenerative capacity (reviewed in Ausoni and Sartore (2009). Upon ventricular resection of the adult zebrafish heart, cardiomyocytes partially dedifferentiate and proliferate to give rise to de novo cardiomyocytes (Jopling et al., 2010; Kikuchi et al., 2010). The recent genetic tracing of EPDCs with a *tcf21* promoter construct suggested that the epicardium is not a cell source for myocardial regeneration after ventricular amputation in the zebrafish (Kikuchi et al., 2011a). Consistent with reports from the mouse, $tcf21^+$ cells do not give rise to all EPDC derivatives and seem to primarily contribute cardiac fibroblasts. Given that *Wt1* fate mapping in a mouse MI-model also revealed a contribution of EPDCs to smooth muscle, it remains plausible that the tcf21-lineage is not a pan-epicardial marker and thus does not label all EPDC descendants during zebrafish regeneration.

To better characterize EPDC differentiation during zebrafish heart regeneration, we sought to perform a cell tracing analysis that bypassed the need for gene-specific fate mapping. We and others recently reported the use of cryoinjury as a regeneration model that simulates the ischemic damage triggered by MI (Chablais et al., 2011; González-Rosa et al., 2011; González-Rosa and Mercader, 2012; Schnabel et al., 2011).

Here, we investigated the fate of EPDCs during regeneration after cryoinjury. We also studied the contribution of EPDCs during regeneration in the context of impaired cardiomyocyte proliferation by analysing the fate of EPDCs grafted to irradiated host hearts. Using this experimental setup we found that upon cryoinjury, EPDCs give rise to fibroblasts, but do not contribute to the myocardial lineage. Indeed, we did not identify any non-cardiomyocyte progenitor cell source within the ventricle capable of differentiating into myocardium. The expression of the secreted molecules *periostin* and *cxcl12a* by EPDCs after injury suggests that, rather than acting as a source of myocardial progenitors, the epicardium promotes cardiomyogenesis and neoangiogenesis through a paracrine action and by forming a cellular scaffold supporting the proliferation of extant cardiomyocytes.

Materials and methods

Zebrafish husbandry

Experiments were conducted with adult zebrafish aged 6–18 months, raised at 3 fish/l. Animal studies were approved by the local ethics committee. All animal procedures conformed to EU Directive 86/609/EEC and Recommendation 2007/526/EC regarding the protection of animals used for experimental and other scientific purposes, enforced in Spanish law under Real Decreto 1201/2005. Fish lines used were the wild-type WIK strain (ZIRC, Eugene, OR, USA), Tg(*cmlc2:nucDsRed*) (Mably et al., 2003), ET-27 (Poon et al., 2010), Tg(*wt1b:eGFP*) (line 1) (Perner et al., 2007), Tg(*β-actin:GFP*) (Higashijima et al., 1997), Tg(*fli1a:GFP)* (Lawson and Weinstein, 2002), Tg(*fli1a:DsRedex*) (Covassin et al., 2009), Tg(*cmlc2:GFP*) (kindly provided by A. Raya, IBEC, Barcelona), Tg(*cd41:GFP*) (Lin et al., 2005), Tg(*ubi:Switch*) (Mosimann et al., 2011) and Tg(*cmlc2:CreER^{T2}*) (Kikuchi et al., 2010). To induce recombination, Tg(*cmlc2:CreER^{T2}/ubi:Switch*) larvae at 48 hpf were exposed to 25 μM 4-OH-tamoxifen for 2 days. The animals were raised to adulthood and used in the experiments described below.

Experimental surgery

The experimental design for transplantations is depicted in Fig. 3A. Cryoinjury was performed as described (González-Rosa et al., 2011). To prevent tissue rejection, host animals were sublethally irradiated with a single dose of 23 Gy, 2 days before transplantation (Langenau et al., 2003; Traver et al., 2004). Hosts were always irradiated unless indicated otherwise. For graft preparation, a freshly dissected cryoinjured donor heart at 3 days postinjury (dpi) was put into a Petri dish containing PBS. The bulbus arteriosus and the atrium were removed, and the apical part of the ventricle cut into 4 pieces. Grafts are subsequently transferred to the pericardial cavity of a freshly operated zebrafish. The graft is usually placed at a distance from the injured area. However, it is not possible to target a specific location, and grafts will eventually attach to an arbitrary region of the cryoinjured ventricle. Hearts were dissected on the desired days posttransplant (dpt), fixed overnight in 4% PFA and processed as described (González-Rosa et al., 2011).

To explore the migratory capacity of the myocardium in the absence of an epicardial layer, two separate procedures were used. In the first, donor hearts were digested at room temperature in 0.5% trypsin and repeatedly passed through a micropipette tip to obtain a single cell suspension. The digestion was then stopped by adding 10% FBS, and the cells were pelleted by centrifugation (1500 rpm, 10 min, 4 °C) and resuspended in 0.05 ml PBS, 10% FBS. Approximately 5 μl were pipetted into the pericardial cavity of a host animal (Fig. S6A).

In the second approach, the epicardium of Tg(*wt1b*:eGFP/*cmlc2*:nucDsRed) donor hearts was removed, following a protocol modified from that used for the generation of recombinant limbs (Ros et al., 2000). Briefly, donor hearts were collected from 3 dpi animals in ice-cold PBS, transferred to a plate containing 0.5% trypsin and digested for 1 h on ice. Digestion was stopped by transferring hearts to a plate containing 10% FBS in PBS.

The epicardium was peeled off with forceps (Fig. S6C). Complete removal of the epicardium was evidenced by lack of GFP expression on the myocardial surface; however, some GFP$^+$ cells located more interiorly were not eliminated. The heart was cut into pieces the same size as for the standard transplantation procedure, and the grafts were transferred to the pericardial cavity of freshly cryoinjured hosts.

Flow cytometry

Hearts collected in ice-cold PBS were digested at room temperature in 0.5% trypsin and repeatedly passed through a micropipette tip to obtain a single cell suspension. Digestion was stopped by adding ice-cold PBS, 10% FBS, and cells were pelleted by centrifugation (1500 rpm, 10 min, 4 °C) and resuspended in 10% FBS in PBS. Dead cells were excluded by staining with 1 μg/ml propidium iodide (Sigma). Cells were analysed for forward scatter, side scatter and GFP fluorescence on a Canto 3L HTS cytometer (Beckton Dickinson). Percentages of GFP$^+$cells were determined by analysing 100,000 cells per sample.

BrdU labelling

For BrdU pulse-chase experiments, animals were anaesthetized in tricaine and injected intraperitoneally with 0.05 ml of a 2.5 mg/ml solution of BrdU dissolved in PBS. Irradiated and control animals were injected once at 3 dpi and were allowed to regenerate until 7 dpi (see scheme in Fig. S3A). Hearts were dissected, fixed and processed as described (González-Rosa et al., 2011).

Immunofluorescence

Immunofluorescence was as described (González-Rosa et al., 2011). The anti-BrdU antibody (BD Biosciences Pharmigen) was used at 1:100, anti-cytokeratin (Dako) at 1:100, anti-collagen type I (SP1.D8, DSHB) at 1:20, anti-myosin light chain kinase (MLCK) (Sigma) at 1:100, anti-myosin heavy chain (MF20, DSHB) at 1:20; anti-GFP (Clontech) at 1:200; and anti-phospho-histone H3 (pH3) (Cell Signaling) at 1:200.

In situ hybridization (ISH) and double ISH/immunohistochemistry on sections

ISH on paraffin sections was performed according to Mallo et al. with minor modifications (Mallo et al., 2000). Probes used were *gfp* (kindly provided by Gómez-Skarmeta), *wt1b* (Perner et al., 2007) *periostin* (Kudo et al., 2004), *cxcl12a* (Haas and Gilmour, 2006) and *collagen 1 alpha 2* (Li et al., 2009). After ISH, sections were fixed, and mounted in 85% glycerol in PBS for imaging. After imaging, sections were washed in PBT and permeabilized by 10 min incubation in 0.5% Triton-X100 (Sigma). Anti-GFP (Clontech) was added at 1:100 dilution and sections incubated overnight. Antibody was detected with the Vectastain Elite ABC staining kit (Vector) and sections mounted in DPX (Sigma).

Imaging

Imaging of sections and dissected whole mount hearts was performed as described (González-Rosa et al., 2011). Data were quantified with ImageJ.

Statistical analysis

Differences between mean values of experimental groups were tested for statistical significance by one-way ANOVA followed by Tukey's honest significant difference test to control for test multiplicity. Model assumptions of normality and homogeneity of variance were checked with conventional residual plots. We did not observe any strong deviation from normality or heterogeneity of variance that would justify the use of a non-parametric test. Statistical significance was assigned at $P < 0.05$.

Results

Epicardial derived cells invade the injured myocardium during zebrafish cardiac regeneration

Previous reports showed that regeneration in the injured zebrafish heart is preceded by the reactivation of epicardial marker genes usually expressed only during development (González-Rosa et al., 2011; Lepilina et al., 2006; Schnabel et al., 2011). Cells expressing epicardial marker genes are found predominantly on the epicardial surface, but can also be found intermingled with the compact layer and in the injured area (IA). Similarly, *tcf21*$^+$-derived cells have also been found in the interior of the regenerated heart at 30 dpi (Kikuchi et al., 2011a). These data suggest that EPDCs migrate into the heart upon injury. However, in the Tg(*wt1b:eGFP*) line (Perner et al., 2007), apart from the expression in the epicardium, some GFP$^+$ cells are also detected intermingled with the compact myocardium and associated with the trabecular endocardium, and the compact myocardial layer of the uninjured heart already contains a subpopulation of *tcf21*$^+$ cells (Kikuchi et al., 2011a and our unpublished data). Therefore the *tcf21*$^+$-derived cells found inside the regenerated ventricle at late stages could be derived from this internal population rather than from epicardial cells on the heart surface.

We wanted to test if epicardial cells can migrate towards and into the injured myocardium. We first carefully analysed the morphological changes undergone by the epicardium upon cardiac damage, using cryoinjury as a model. We found that not only did the gene expression profile of epicardial cells change, but also that their morphology was altered very rapidly upon injury. In control situations, epicardial cells have a flattened, epithelial morphology, revealed by the expression of GFP in the trap line ET27 (Poon et al., 2010), labelling the epicardium (Fig. 1A, A′). Only a few *wt1b:*eGFP$^+$ cells can be detected on the heart surface (Fig. 1B, B′). Notably, these cells are smaller than the other epicardial cells and do not have the same epithelial structure. Cryoinjury leads to the destruction of all cell types in the IA, including the epicardium. During the first hours postinjury, epicardial cells from non-injured areas lose their cell adhesions (Fig. 1C–C′). Cells expressing *wt1b:*eGFP$^+$ accumulate at the injury site (Fig. 1D). These cells have cytoplasmic extensions and lamellipodia, indicating motility, and some were found intermingled with the subepicardial tissue (Fig. 1D′). Since there is almost no detectable proliferation at this stage (data not shown), these cells are probably derived from epicardial cells that reexpress *wt1b* and migrate to the injury site, rather than from proliferation of the pre-existing *wt1b*-positive population.

To further analyse the ability of epicardial cells to invade the myocardium during adult zebrafish heart regeneration, we next compared the distribution of GFP protein and mRNA expression in cryoinjured Tg(*wt1b:eGFP*) ventricles at 7 days post injury (7 dpi) (Fig. 1E–H). We used the immunodetection of GFP protein as a short-term tracer of cells that express or have recently expressed *gfp* mRNA. In situ hybridization followed by immunohistochemistry

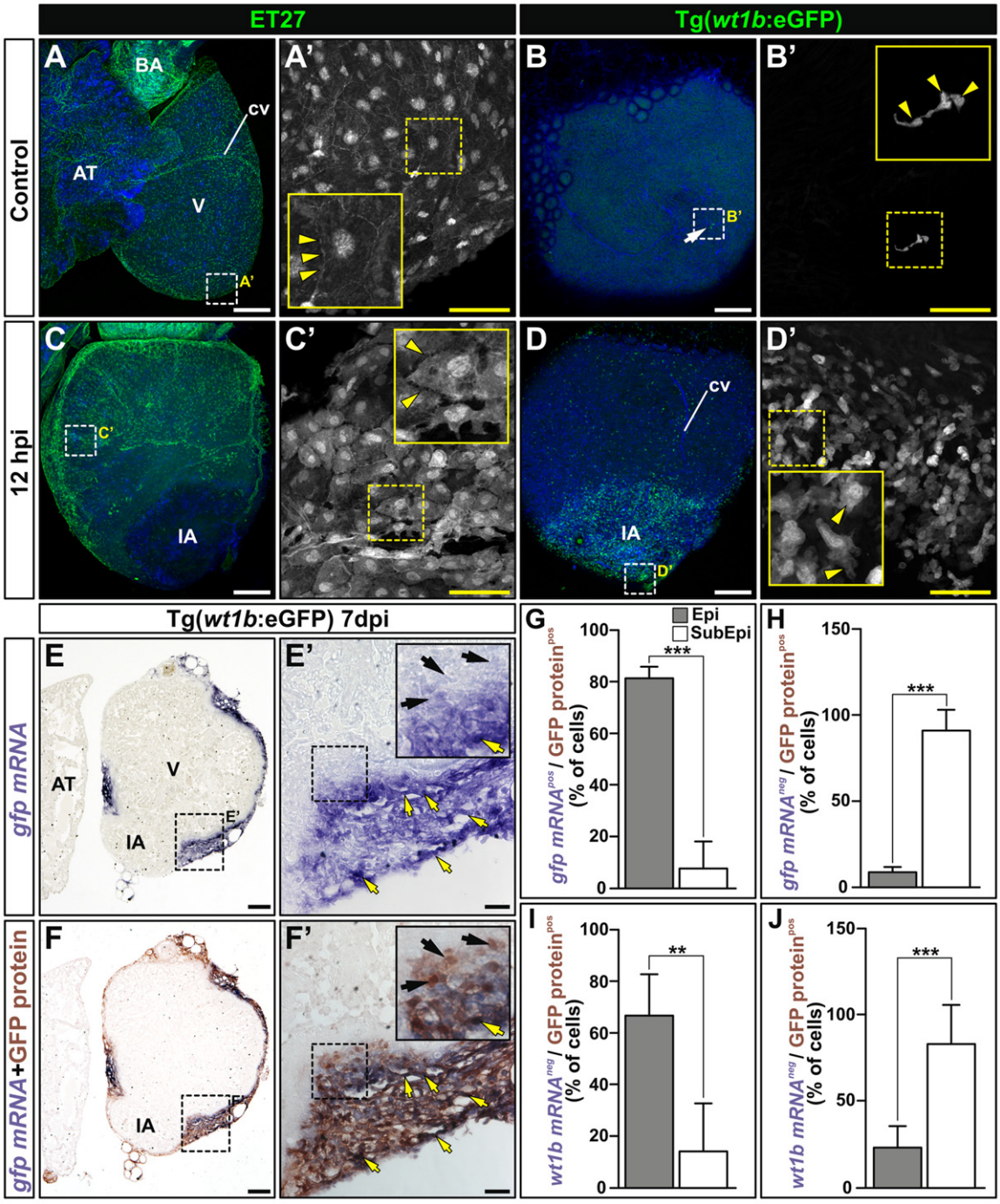

Fig. 1. Epicardial derived cells migrate upon cryoinjury. (A–D) Whole-mount imaging of dissected control and cryoinjured hearts (12 h postinjury: hpi) from the ET27 and Tg(*wt1b*:*eGFP*) lines. Nuclei are counterstained with DAPI (blue). A′–D′ are zoomed images showing the GFP channel in the boxed areas in A–D. Arrows marks GFP$^+$ cells, arrowheads mark morphological cell features. (E–J) Comparison of the expression domains of *wt1b*:GFP protein and *gfp* and *wt1b* mRNA. (E,E′) Full view and zoomed images of *gfp* in situ hybridization on a Tg(*wt1b*:*eGFP*) heart section at 7 dpi. Yellow arrows mark cells expressing *gfp* mRNA, black arrows mark cells devoid of *gfp* mRNA expression. (F,F′) Same sections in E,E′ after anti-GFP immunohistochemistry. Yellow arrows mark cells coexpressing GFP protein and *gfp* mRNA, black arrows mark cells only expressing GFP protein. (G) and (H) Percentage of cells coexpressing *gfp* mRNA and protein (G) or only protein (H). Note that while most epicardial cells coexpress *gfp* mRNA and protein, most subepicardial cells only express GFP protein. (I) and (J) Percentage of cells coexpressing *wt1b* mRNA and GFP protein (I) or only protein (J). Results are similar to those in G and H. Data are means of cell percentages ± S.D. counted on 1–3 heart sections per specimen from 2–5 specimens (***$P < 0.001$; **$P < 0.01$; one-way ANOVA followed by Tukey's honest significant difference test; 100–150 cells counted per section). AT, atrium; BA, bulbus arteriosus; cv, coronary vessel; dpi, days postinjury; IA, injured area; ISH, in situ mRNA hybridization; V, ventricle. Bars, 200 μm (full views) and 50 μm (magnifications).

revealed that most GFP$^+$ cells from the thickened epicardial layer co-express *gfp* mRNA (Fig. 1G). In contrast, most GFP$^+$ cells located in the more internal layers and compact myocardium did not coexpress *gfp* mRNA (Fig. 1H), suggesting that the GFP$^+$ cells in these locations came from an epicardial position. We obtained similar results by comparing the distribution of *wt1b* mRNA and GFP protein (Fig. S1 and Fig. 1I and J). These results support the idea that epicardial cells transiently reexpress *wt1b* during the initial stages of regeneration, subsequently downregulating expression during migration into the myocardium.

Interestingly, *wt1b*:eGFP$^+$ cells were often found closely associated with coronary vessels in cryoinjured hearts (Fig. 2A,A′). Association with the coronary vessel wall was observed even at very late stages of regeneration (Fig. 2B,B′). We did not detect *wt1b*:eGFP$^+$ coronary vascular smooth muscle or endothelial cells either in control hearts or upon cryoinjury (Fig. 2C–D′), suggesting that *wt1b*:eGFP$^+$ cells give rise to perivascular fibroblasts. Furthermore, we found that *wt1b*:eGFP$^+$ cells expressed the fibroblast marker genes *collagen-1 alpha 2* and *periostin* at 3 dpi (Fig. 2E–H′). Control hearts expressed undetectable levels of these genes (Fig. S2), strongly suggesting that epicardial cells differentiate into fibroblasts upon cardiac injury.

The mouse epicardium has been suggested to be a source of myocardial progenitors during development and potentially also during repair (Cai et al., 2008; Smart et al., 2011; Zhou et al., 2008). To assess whether *wt1b*:GFP$^+$ cells can give rise to cardiomyocytes in the zebrafish, we analysed the coexpression of *wt1b*:eGFP$^+$ cells with the late cardiomyocyte differentiation marker myosin heavy chain (MHC). Immunohistochemistry was performed on heart sections from control as well as cryoinjured adult hearts. We did not detect MHC expression in *wt1b*:eGFP$^+$ cells of cryoinjured ventricles at any stage analysed (ranging from 1 to 130 dpi) (Fig. 2A–B′ and González-Rosa et al., 2011). This might indicate that *wt1b*:eGFP$^+$ cells do not give rise to cardiomyocytes, but could also reflect reporter gene downregulation during differentiation.

Tissue transplantation provides an unbiased method for studying EPDC migration

Recent evidence suggests that the epicardium is a heterogeneous cell population. To examine the fate of all epicardial derived cells, we designed a cell tracing assay based on tissue transplantation using GFP expressing donors. By using genetically labelled reporter lines as donors, this system avoids the problem of promoter downregulation, allowing permanent labelling of transplanted cells (Fig. 3A). Donor hearts are cryoinjured and at 3 dpi the ventricles cut into small pieces. At this stage, the epicardium has increased its thickness (González-Rosa et al., 2011). Each graft is transplanted into the pericardial cavity of a freshly-cryoinjured wildtype heart of a previously irradiated fish, and allowed to adhere to the ventricular surface. We have noticed that grafts preferentially adhere to the ventricular apex (65% of grafts analyzed; $n=23$). However, this does not signify a preferred adherence near the site of injury, since grafts transplanted to uninjured control hearts also attached at an apical position ($n=5$). Grafts usually adopted a spherical morphology, whereby the myocardium is covered by an epicardial layer. The size of the graft was around 20% of the size of the host ventricle (Fig. 3B). By using the reporter lines Tg(*wt1b:eGFP*), Tg(*fli1a:GFP*) and Tg(*cmcl2:GFP*) as donors, we could estimate the composition of the graft and found that it was composed of epicardial and endothelial cells as well cardiomyocytes (Fig. 3C).

To further characterize the transplantation method, we used Tg(β-*actin*:*GFP*) donors, which express GFP under the β-actin promoter (Higashijima et al., 1997), thus allowing permanent labelling of transplanted cells (Fig. 3D–E″). GFP$^+$ cells were monitored at 4 days posttransplantation (dpt). Grafts transplanted into non-injured wildtype hearts had a limited capacity to adhere to the myocardial surface ($n=6$ of 15 transplants). Importantly, no GFP$^+$ cells were detected on the surface of the uninjured host ventricle (Fig. 3D–D″). In contrast, tissue grafted to cryoinjured hearts adhered effectively ($n=29$ of 31 transplants), and GFP$^+$ cells were readily observed on the myocardial surface and inside the myocardium (Fig. 3E–E″). The effect of irradiation on host cell proliferation was analysed by pulse-chase assay (see scheme in Fig. S3A). As reported previously, cryoinjury massively increased cell proliferation in the hearts of non-irradiated animals (Fig. S3B,B′). In contrast, few BrdU-positive cardiomyocytes were detected in cryoinjured ventricles of irradiated animals (Fig. S3C,C′). Moreover, since γ-irradiation arrests the cell-cycle in G2 (Wendt et al., 2006), these BrdU-positive cardiomyocytes could have incorporated BrdU during S phase without subsequently dividing. This was confirmed by detecting cells in the G2/M transition and M phase by immunohistochemistry with anti-phospho-histone H3 (pH3) antibody (Hendzel et al., 1997). Sections of non-irradiated hearts contained several pH3-positive cells, including cardiomyocytes (Fig. 3F–F′). In contrast, although the graft contained many pH3-positive cells (Fig. 3G–G′), there was almost no staining in irradiated host tissue, and no dividing cardiomyocytes were detected in irradiated animals (Fig. 3G″; $n=6$ analysed hearts). Thus by effectively inhibiting host regenerative capacity, transplantation to irradiated hosts provides a valid system for detecting low frequency myocardial differentiation by EPDCs.

To evaluate the suitability of this technique for tracking EPDCs we used the Tg(*wt1b:eGFP*) line as the donor. In these experiments, many *wt1b*:GFP$^+$ cells migrated towards the host ventricle ($n=12$; Fig. 4A,A′). Cross-sections revealed cells forming a thickened epicardial layer on the cryoinjured heart (Fig. 4B and C). Importantly, some EPDCs extended protrusions towards the compact layer of the host myocardium (Fig. 4D), and others were found in the interior of the IA and compact myocardium (Fig. 4E and F). To assess the degree of overlap between the expression of *wt1b*:GFP and other epicardial markers such as *tbx18* we quantified the number of cells double positive for GFP and *tbx18* on tissue sections (Fig. 4G–I). While the populations were broadly overlapping, there was a small population of GFP$^+$ cells not expressing *tbx18*, again revealing heterogeneity in gene expression among EPDCs.

The use of donor hearts from transgenic lines expressing GFP under the control of ubiquitous promoters such as β-actin (Higashijima et al., 1997) or ubiquitin (Mosimann et al., 2011) ensures permanent labelling of grafted cells, avoiding the limitations of using reporter lines for a non-ubiquitous gene. In cryoinjured Tg(β-*actin:*GFP) hearts, GFP was expressed at high level in all cardiomyocytes, at low level in all epicardial cells, and at a lower level in all other cell types, with some circulating cells showing no expression (Traver et al., 2003) (Fig. 4J–L). In the Tg(*ubi:loxP-GFP-loxP-mCherry; cmlc2:GFP*) line (Mosimann et al., 2011), called Tg(*ubi:Switch*), GFP was expressed homogeneously in all cardiac cell types at 3 dpi (Fig. 4M–O). At 3 dpt, β-*actin*:GFP$^+$ cells had spread over the host myocardium, covering the IA (Fig. 4P), and could also be detected inside the IA (Fig. 4Q and R). Co-staining for GFP with *tbx18* showed that approximately 50% of grafted cells were *tbx18*$^+$, revealing that the graft is enriched in EPDCs (Fig. 4S–U). We also performed immunohistochemistry against cytokeratin (CK), a marker previously used to detect epicardial cells and EPDCs shortly after EMT (Vrancken Peeters et al., 1995). β-*actin*:GFP$^+$ cells in host tissue were cytokeratin$^+$, indicating an epithelial origin ($n=42$ cells from 3 animals analysed; Fig. S4A–C). As expected for epicardial cells shortly after EMT, the level of CK expression in the β-*actin*:GFP$^+$ cells was significantly lower than in epithelial cells (Fig. S4D). These results demonstrate that transplantation of epicardial-cell-enriched cardiac grafts into irradiated host hearts is a valuable tool for the study EPDC migration and differentiation.

Epicardial cells do not contribute to the myocardial lineage after cryoinjury

If transplanted epicardial β-*actin*:GFP$^+$ cells give rise to myocardium, GFP$^+$ cells expressing cardiomyocyte markers should be found

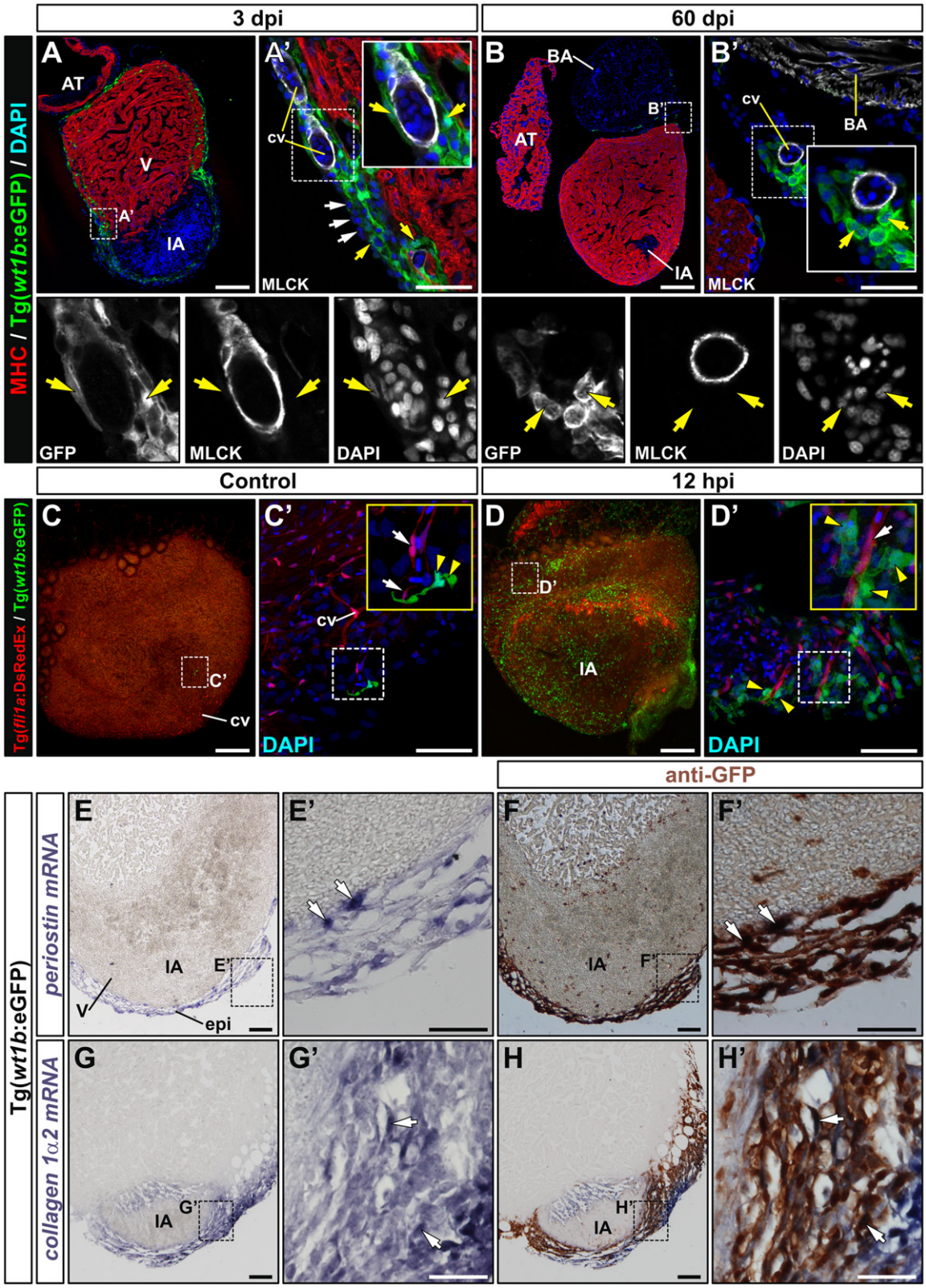

Fig. 2. *wt1b*:eGFP cells give rise to perivascular cells and express fibroblast marker genes upon cryoinjury. (A) and (B) Immunohistochemistry on sections of cryoinjured Tg(*wt1b:eGFP*) hearts, using antibodies against myosin heavy chain (red) to detect myocardium and GFP (green) to detect *wt1b*:eGFP$^+$ cells. A′–B′ are zoomed images of boxed areas in A and B, additionally showing myosin light chain kinase (MLCK, white) to detect smooth muscle cells surrounding coronary endothelial cells. The bottom row shows three separate channels for the zoomed regions. (A′) At 3 dpi, GFP$^+$ cells surround but do not co-localize with MLCK$^+$ cells. Note that not all epicardial cells are GFP$^+$ (white arrows). (B′) At 60 dpi the few GFP$^+$ cells visible in the cryoinjured heart are again associated with coronary vessels. Yellow arrows mark GFP$^+$ cells. (C) and (D) Whole mount fluorescence imaging in control (C–C′) and 12 hpi cryoinjured hearts (D,D′) from the Tg(*wt1b:eGFP*)/Tg(*fli1a:DsRedEx*) line. Zoomed views show DAPI nuclear counterstaining. Endothelial cells are visible by DsRed fluorescence. White arrows mark endothelial cells and yellow arrowheads highlight *wt1b*:GFP$^+$ cells in close apposition. (E–H) Sections of cryoinjured Tg(*wt1b*:eGFP) hearts (3 dpi) hybridized with riboprobes for *periostin* and *collagen 1 alpha 2* mRNAs. In panels F and H, sections were immunostained for GFP after ISH. Arrows mark GFP$^+$ cells co-labelled with the ISH probe. Abbreviations are as in previous figures. A′–H′ are zoomed views of the boxed areas in E–H. Bars, 200 μm (full views), 50 μm (magnifications).

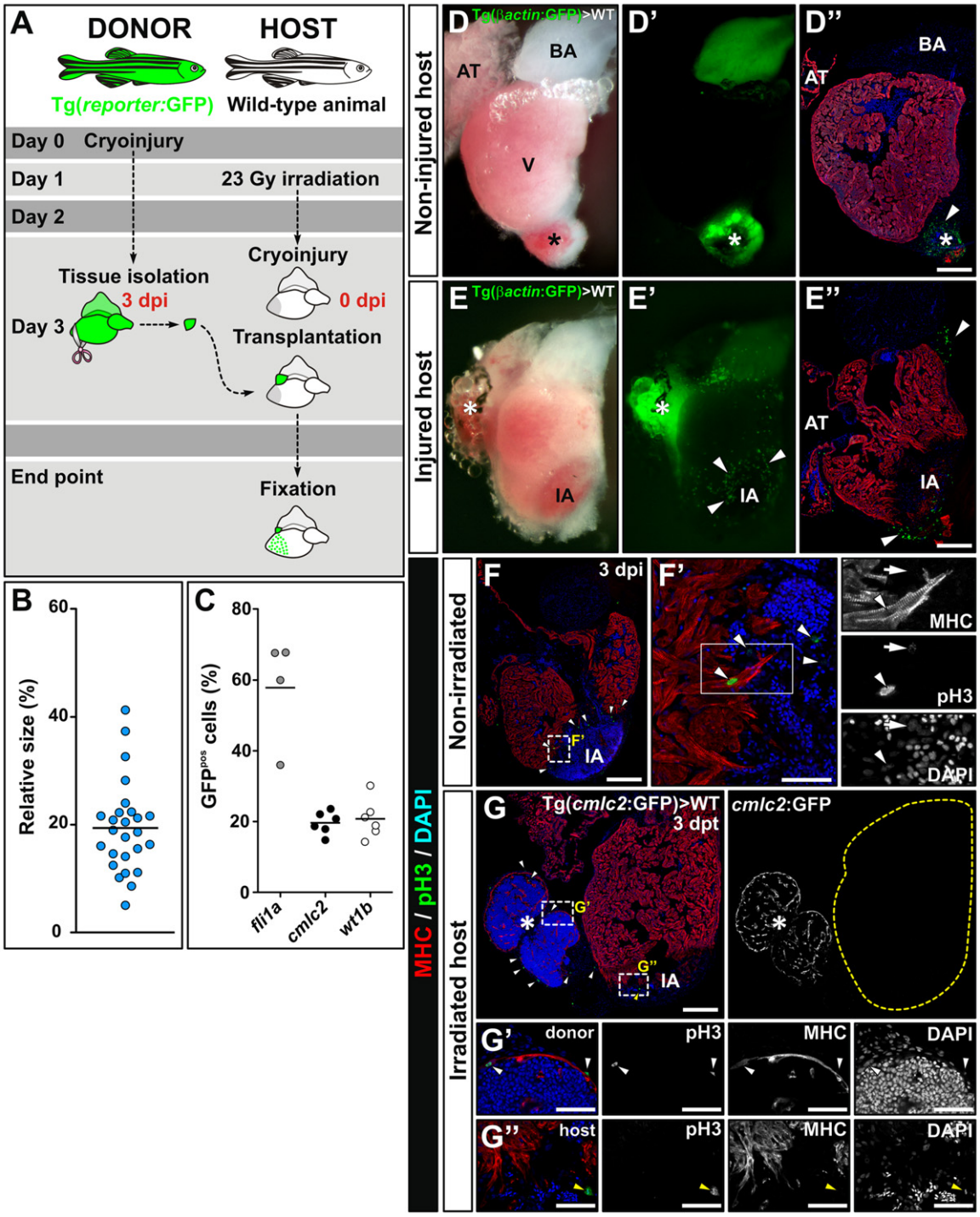

Fig. 3. Cardiac tissue transplantation method for the study of cellular contribution during zebrafish heart regeneration. (A) Experimental scheme. Donor hearts from a transgenic reporter fish line were cryoinjured and dissected at 3 dpi. Cardiac tissue explants containing epicardium were transplanted into freshly-cryoinjured hearts of irradiated wild type fish. Host hearts were fixed at different stages and the contribution of grafted cells to the regenerated tissue analysed. (B) Quantification of the size of the grafted tissue. The plot shows the size of 26 grafts at 3 days posttransplantation (dpt), each graft being represented by a circle as the percentage relative to the host ventricle. The horizontal bar indicates the mean % of the graft size. (C) Cell composition of grafts. The percentage of cells expressing endothelial/endocardial, myocardial and epicardial markers within each graft was estimated by FACS of cells from 4 to 6 donors before transplantation. Horizontal bars indicate the mean % of cells. (D–E′) Bright field and fluorescence images of hearts at 4 dpt. (D–D″) Transplantation of a Tg(β-*actin:GFP*) graft to an uninjured wildtype (WT) heart did not result in contribution of graft-derived cells to the host. (D) Bright field whole mount view. (D′) GFP fluorescence in the specimen in D: while grafted tissue (asterisk) is strongly GFP^+, no GFP^+ cells are found on the surface of the host heart (the signal in the bulbus arteriosus is autofluorescence). (D″) Immunohistochemistry on sections, using antibodies to myosin heavy chain (MHC) to label myocardium (red) and GFP to label grafted cells (green) reveals green cells in the graft but not in the host heart. Cell nuclei are labelled with DAPI (blue). (E–E″) After grafting Tg(β-*actin:GFP*) tissue to a cryoinjured heart, GFP^+ cells attach to and spread over the surface of the host myocardium. Views are as in D–D″. Immunohistochemistry on sections reveals β-*actin:*GFP cells inside the host heart. Arrowheads in D″, E′ and E″ mark GFP^+ cells. (F–G″) Effect of irradiation on cell proliferation. (F–F′) Immunohistochemistry on wildtype heart sections at 3 dpi, revealing phospho-histone H3 (pH3) staining in green, myosin heavy chain (MHC) in red and nuclear counterstain with DAPI (blue). F′ shows a zoomed view of the boxed area in F, and separate channels of the central area are shown to the right. Arrowheads mark numerous $pH3^+$ cells close to the IA, and the white arrow marks a mitotic cell with punctuated pH3 staining (late G2). (G–G″) Staining as in F on a cryoinjured heart from an irradiated wildtype fish grafted with tissue from the cryoinjured heart of Tg(*cmcl2:GFP*) donor fish at 3 dpt. The panels show a whole-mount view (G) and zoomed views of boxed areas (G′ and G″). While the graft contains numerous $pH3^+$ cells, including cardiomyocytes (G′), the irradiated host heart is almost devoid of $pH3^+$ cells (G″). pH3-positive cells from the graft are marked by white arrows; that in the irradiated host is marked by a yellow arrow. G′ and G″ represent zoomed views of boxed regions in G showing merged and single channel views. Note the pH3-positive cardiomyocyte in G′. Asterisks mark the graft. Abbreviations as in previous figures. Bars, 200 μm (full views) and 50 μm (magnifications).

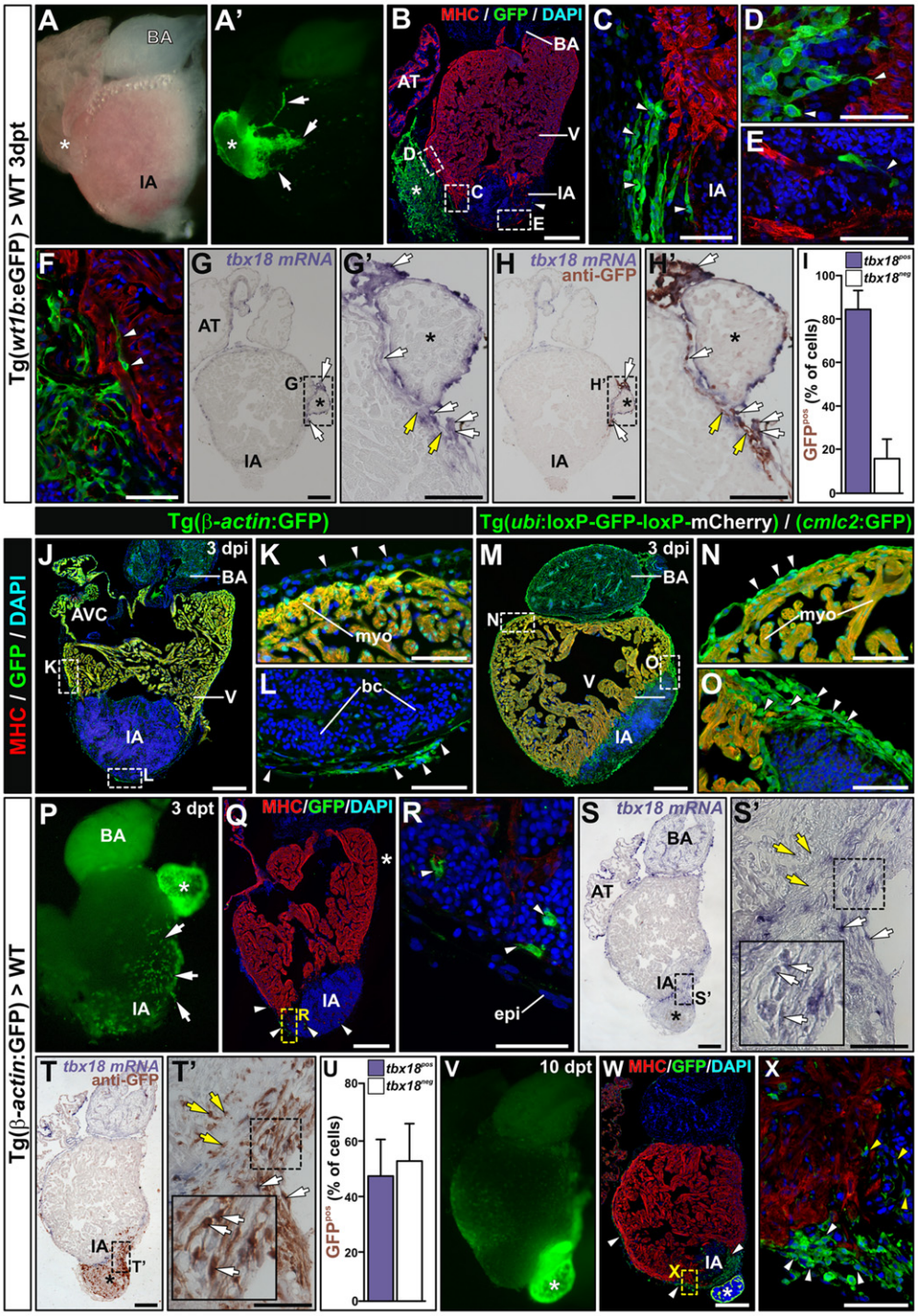

Fig. 4. Transplantation assays allow the study of pan-EPDC migration and differentiation during cardiac regeneration. (A,A′) Brightfield and fluorescence images of a freshly-dissected 3 dpt wildtype heart transplanted with a Tg(*wt1b:eGFP*) graft. Arrows mark GFP$^+$ extensions of the graft migrating over the host. (B) Whole heart cross-section showing the Tg(*wt1b:eGFP*) graft adhered to the host. (C–F) Zoomed views of boxed areas in B (C–E) or areas from adjacent sections (F), showing the epicardial sheet covering the IA (C), protrusions of *wt1b*:eGFP$^+$ cells extending towards the host myocardium (D), a migratory *wt1b*:eGFP$^+$ cell inside the IA (E), and GFP$^+$ cells intermingled with host cardiomyocytes (F). Arrowheads mark GFP$^+$ cells. (G,G′) Whole-mount and zoomed views of an in situ hybridization with a *tbx18* riboprobe on a section of a transplanted heart at 3 dpt. (H,H′) Section in G after immunohistochemistry with anti-GFP. (I) Percentage of GFP$^+$/*tbx18*$^+$ and GFP$^+$/*tbx18*$^-$ cells in the host. Data are means of cell percentages ± S.D. counted on 2–3 heart sections per specimen from 5 specimens (80 cells counted per section). (J-O) Immunohistochemistry on sections of Tg(*-actin:GFP*) (J-L) and Tg(*ubi:loxP-GFP-loxP-mCherry*)/(*cmlc2*:GFP) hearts (M-O). Antibodies/stains used are indicated to the left of the panels. Arrowheads mark epicardial cells. (P-X) Tg(*-actin*:GFP) > WT transplants at 3 and 10 dpt. Arrowheads mark graft-derived cells. (P) Whole-mount fluorescence view at 3 dpt. Arrows point to grafted cells on the surface of the host heart. (Q) Immnohistochemistry on a sagittal section of the heart shown in P. (R) Zoomed view of boxed area in Q revealing cells that migrated into the IA. (S,S′) Whole-mount and zoomed views of in situ hybridization with *tbx18* on a Tg(β-*actin:GFP*) > WT heart section. (T,T′) Section as in S and S′ after immunostaining for GFP. Note the strong overlap of *tbx18* and GFP expression. (U) Percentage of GFP$^+$/*tbx18*$^+$ and GFP$^+$/*tbx18*$^-$ cells in the host. Data are means of cell percentages ± S.D. counted on 3 heart sections per specimen from 3 specimens (50 cells counted per section). (V) Full view of a freshly dissected heart at 10 dpt. (W) Immunohistochemistry on a sagittal section of the heart shown in V. Antibodies used are specified in the panel. (X) Zoomed view of boxed area in V, revealing cells forming an epicardial cap over the IA. Note that no GFP$^+$/MHC$^+$ cells are detected. In all panels, asterisks mark the graft or its position in a consecutive section. In G–H′ and S–T′ white arrows label GFP$^+$/*tbx18*$^+$ cells and yellow arrows GFP$^+$/*tbx18*$^-$ cells. AVC, atrioventricular canal, epi, epicardium. Other abbreviations are as in previous figures. Bars, 200 μm (full views) and 50 μm (magnifications).

in the regenerating myocardium of the host. Co-staining with GFP and MHC antibodies at 3 and 10 dpt revealed that, although graft-derived cells contributed to the host heart, they did not express sarcomeric proteins, suggesting that they have not differentiated into mature cardiomyocytes (Fig. 4R,V–X).

To define the later fate of graft- derived EPDCs, we conducted a long-term study of transplanted hearts. For donors we used a double transgenic line Tg(*cmlc2:CreER^{T2}*/*ubi:Switch*) (Kikuchi et al., 2010; Mosimann et al., 2011) treated with 4-OH-tamoxifen at larval stages to induce recombination of the reporter construct in all cardiomyocytes. Upon recombination, non-cardiomyocytes express only GFP, while cardiomyocytes express mCherry as well as GFP, which is present in the transgenesis cassette for selection and is not removed by recombination. This approach thus allows us to distinguish between host tissue (GFP$^-$ and mCherry$^-$), myocardium regenerated by graft-derived cells of cardiomyocyte origin (MHC$^+$, GFP$^+$ and mCherry$^+$) and non-cardiomyocyte origin (MHC$^+$, GFP$^+$, mCherry$^-$) as well as other non-myocardial cell types derived from the graft (MHC$^-$ and GFP$^+$ Fig. 5A). Of the 20 host animals used for this experiment only 5 survived to 30 dpt, possibly as a result of the experimental procedures, including irradiation. Although regeneration is normally very advanced by 30 dpi, three irradiated specimens showed no signs of healing at 30 dpt and the IA was still clearly visible (Fig. 5B). Interestingly, in these hearts there was also little or no contribution of graft cells to the host heart (Fig. 5B′–C). In contrast, in two specimens in which the graft was clearly visible and graft-derived cells had contributed extensively to the host heart, there was little sign of injury in the freshly dissected heart (Fig. 5D–D″) and the IA was surrounded by myocardium. Immunohistochemistry confirmed the accumulation of many graft-derived cells at the IA and the presence of healed myocardium around the IA (Fig. 5E). These results show that grafted cells persist in the host tissue and intermingle with the host cells. Although the graft was still visible and contained mCherry$^+$ cardiomyocytes, none of them had migrated into the host tissue (Fig. 5D″). Importantly, none of the grafted GFP$^+$ cells gave rise to fully differentiated cardiomyocytes (Fig. 5E–F′). Thus these results also suggest that even though host cardiomyocyte proliferation is impaired by irradiation, EPDCs do not represent a cardiomyocyte progenitor source during regeneration.

Immunohistochemistry revealed that most grafted cells express fibroblast markers at 30 dpt. Cells surrounding the inner IA border were MLCK-positive, suggesting that they adopted a myofibroblast-like phenotype (Fig. 5G–G′). Those forming a more peripheral ring around the remaining IA were positive for collagen 1 alpha 1 (Fig. 5H–H′). In addition, some grafted cells that had migrated into the host heart close to the graft formed coronary vessels or surrounded coronary vessel walls, adopting a pericyte-like morphology (Fig. 5I–I′ and data not shown).

Although a high percentage of the cells invading the host myocardium at 3 dpi are EPDCs, it cannot be assumed that all grafted cells present at 30 dpi are of epicardial origin. It is furthermore possible that the unexpected absence of graft-derived cardiomyocytes in the host heart at 30 dpt reflects elimination of such cells during regeneration. An alternative explanation is that different cell types might not have the same ability to migrate from the graft to the host tissue. Use of Tg(*fli1a:eGFP*) donors revealed spouting of vessels from the graft at 3 dpt, indicating a contribution from graft endothelium ($n=4$, Fig. S5A–A′). In contrast, using Tg(*cmlc2:eGFP*) donors we did not detect any contribution from graft myocardium ($n=4$, Fig. S5B–B′). To determine the possible contribution of graft-derived circulating cells, we used the Tg(*cd41:GFP*) line as a donor, in which thrombocytes and hematopoietic stem cells are GFP$^+$. *cd41*:GFP$^+$ cells have been been shown to migrate towards the IA (Kim et al., 2010). However, we found very little migration of graft-derived *cd41*:GFP$^+$ cells into the host heart ($n=5$; Fig. S5C–C′). Examination of Tg(*fli1a:eGFP*) transplants at 30 dpt did not reveal a major contribution of grafted *fli1a*:eGFP$^+$ endothelial cells to the host ($n=4$; Fig. S5D–D′), suggesting that the small sprouts detected at 3 dpt connect the graft to the host coronary circulation but make little contribution to the regeneration of the host heart.

The lack of graft-derived cardiomyocytes inside the host suggests that differentiated cardiomyocytes have a limited migratory capacity in this assay, possibly due to their inability to cross the epicardial cap formed between the host and graft tissue. To overcome this, we injected a suspension of cells from a cryoinjured Tg(*cmlc2:eGFP*) donor directly into the host pericardial cavity (Fig. S6A). We did not find any contribution of these cells to the host at 7 dpt ($n=6$, Fig. S6B–B′). In a second approach, we peeled off the epicardium from cryoinjured donor Tg(*cmlc2:nucDsRed*/*wt1b:eGFP*) hearts before transplant. Elimination of the epicardium was monitored by GFP fluorescence. The few interiorly located EPDCs were not removed (Fig. S6C), and these remaining cells were enough to proliferate and encapsulate the grafted tissue. Again, cardiomyocytes were not found in the host tissue ($n=6$; Fig. S6D–D″).

These results support the idea that EPDCs are the main cell type migrating from the graft into the host. Our results further suggest that EPDCs play a dual role during regeneration. In the short term, they contribute to the formation of a transient fibrotic scar. This population disappears after complete regeneration, presumably through apoptosis. However, *wt1b*:GFP$^+$ cells also give rise to a population of pericyte-like cells which persist even after complete regeneration.

Grafted cells promote zebrafish heart regeneration through a paracrine action

The long-term transplant experiments indicate that grafted cells improve host regeneration after cryoinjury. Apart from contributing structurally to the scar, grafted cells might also exert a trophic effect on host cardiac tissue. During development, the epicardium promotes myocardial development by secreting trophic factors such as retinoic acid (RA) and fibroblast growth factors (Sucov et al., 2009). Recent reports suggest that the epicardium might also promote cardiomyocyte proliferation during regeneration through a similar paracrine mechanism. In the regenerating heart, the epicardium reexpresses the retinoic acid synthesizing enzyme *aldh1a2* (Lepilina et al., 2006), and RA has been shown to be required for zebrafish cardiomyocyte regeneration (Kikuchi et al., 2011b). As mentioned before we found that, in addition to *aldh1a2,* the injured epicardium also reexpressed *periostin*, which encodes an extracellular matrix protein that promotes cardiomyocyte proliferation and cardiac repair after MI (Kuhn et al., 2007) (Fig. 2E–F′).

To assess whether grafted cells promote neoangiogenesis via a paracrine mechanism, we transplanted Tg(β-*actin:GFP*) grafts onto non-irradiated Tg(*fli1a:DsRedEx*) cryoinjured hearts (Fig. 6A and B). Numerous vessel sprouts could be observed migrating into the graft (Fig. 6C–C″). We also examined the expression of the key proangiogenic chemokine Cxcl12, whose expression is upregulated after MI (Takahashi, 2010). While *cxcl12a* was not expressed in untreated control hearts (Fig. S2), *cxcl12a* mRNA was strongly upregulated in *wt1b*:eGFP$^+$ cells at 4 dpi, suggesting that the epicardium secretes this proangiogenic factor (Fig. 5D–E′).

Our results suggest that EPDCs might support myocardial regeneration by supporting cardiac cell proliferation and neoangionesis through the secretion of trophic factors and contributing cells to the regenerating coronary vasculature.

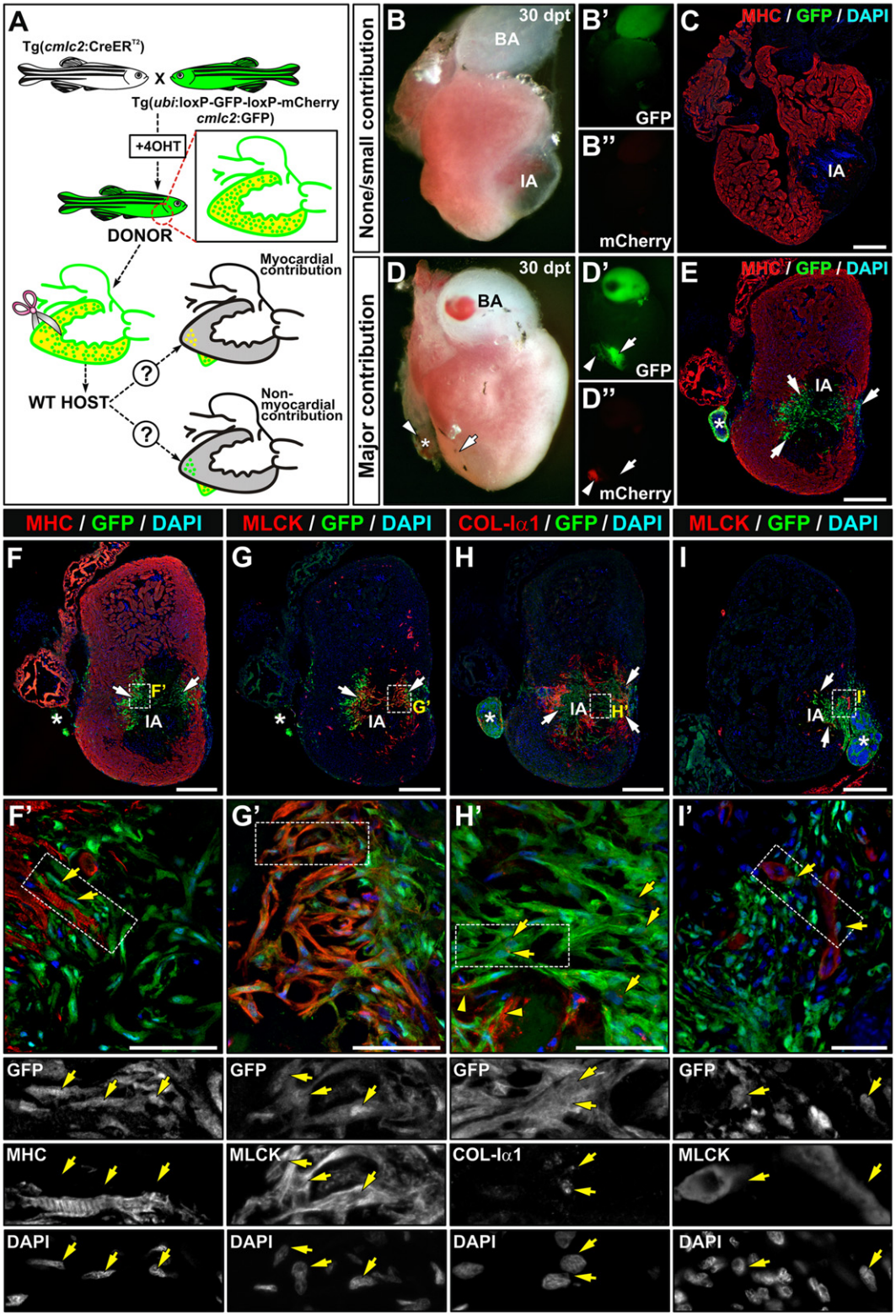

Fig. 5. Long term follow up of transplants. (A) Scheme of the experimental procedure and possible outcomes of transplantation assays using the Tg(*cmlc2:CreERT2*)|(*ubi*:loxP-*GFP*-loxP-*mCherry*)|(*cmlc2:GFP*) line as donor. Recombination was induced at larval stages to induce mCherry expression in cardiomyocytes. Grafts of transgenic fish, expressing mCherry and GFP in the myocardium and GFP only in all other cells, were transplanted onto cryoinjured wildtype hearts. If grafted myocardium contributes to the regenerating myocardium, GFP/DsRed cells will be found in the host heart. If any non-myocardial donor cell contributes to the regenerated host myocardium, GFP^+ cardiomyocytes would be found in the host heart. (B–B″) Freshly dissected heart revealing non-detectable graft at 30 dpt, revealed by the absence of signals for GFP (B′) and mCherry (B″). Note the presence of a large IA and the absence of regeneration. (C) Immunohistochemistry on a section of the same heart as in B. Antibodies used are indicated in the panel. Note that no GFP^+ (graft-derived) cells can be found inside the host heart. (D–D″) Freshly dissected heart revealing no signs of injury at 30 dpt and a visible graft: the host heart contains graft-derived cells (D′) but no graft-derived cardiomyocytes (D″). (E) Immunohistochemistry on a section of the same heart as in D. Antibodies used are indicated in the panel. Many GFP^+ cells are detected inside the host and accumulate at the borders of the remnant IA (arrows). Note the partial regeneration of the myocardial wall. Arrowheads mark graft, arrows mark graft-derived GFP-positive cells. (F–I′) Immunohistochemistry on sections with antibodies indicated above the panels; panels F′–I′ show zoomed views of boxed areas. There is no collocalization of GFP with the myocardial marker MHC, but broad overlap with MLCK and Col-1α1. Asterisks mark the graft or its position in a consecutive section. Bars, 200 μm (full views) and 50 μm (magnifications).

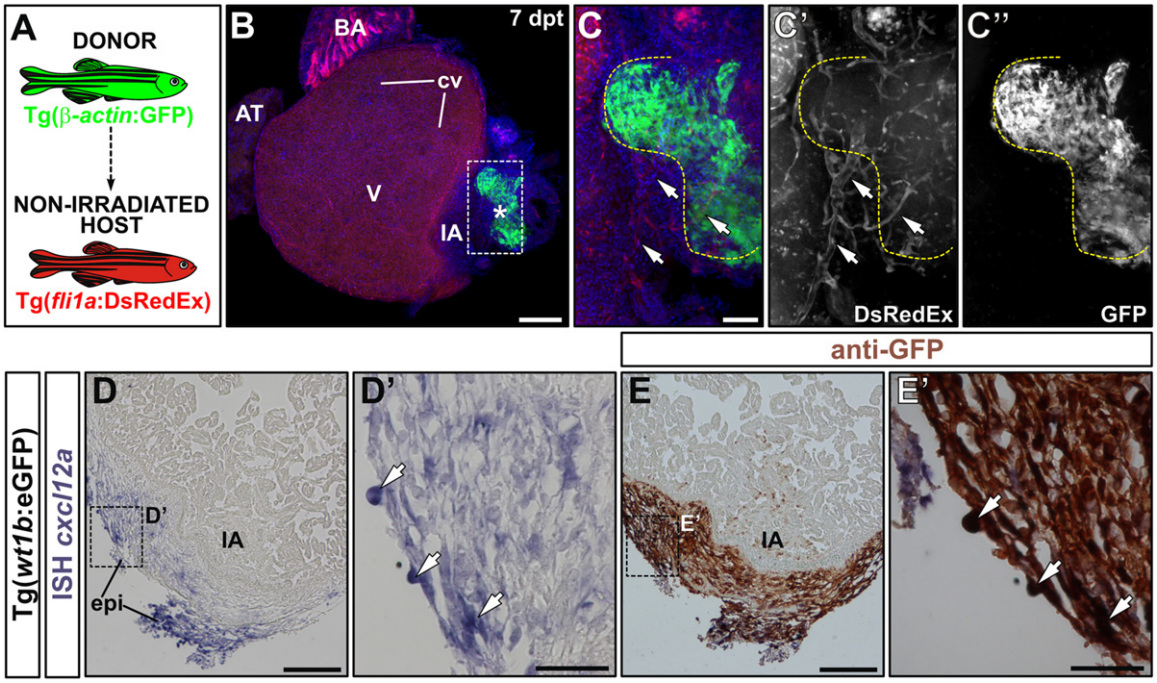

Fig. 6. Grafted cells promote neoangiogenesis and *wt1b*:GFP cells express *cxcl12a*. (A) Experimental scheme. Grafts were derived from Tg(β-*actin:GFP*) animals and implanted in non-irradiated Tg(*fli1a*:DsRedEx) cryoinjured hosts. (B–C″) Whole mount (B) and zoomed views of boxed areas (C,C″). GFP is shown in green, DsRed fluorescence is shown in red and DAPI nuclear counterstain in blue. C′ shows DsRed fluorescence only. Note the presence of host-derived capillaries within the graft. Arrows mark coronary vessels. (D,D′) Section of cryoinjured Tg(*wt1b*:eGFP) hearts (3 dpi) hybridized with a riboprobe against *cxcl12a*. (E,E′) Same section immunostained for GFP after ISH. D′ and E′ show zoomed views of the corresponding boxed areas in E and D. Arrows mark GFP$^+$ cells co-labelled with the ISH probe. Abbreviations as in previous figures. Bars, 200 μm (full views), 50 μm (magnifications).

Discussion

Transplants provide a tool for the study of cell fate during heart regeneration

Transplantation of tissue grafts has been widely used in developmental biology and regeneration to tackle problems of cell fate and cell-autonomous versus non-autonomous gene function (e.g., Kragl et al., 2009; Rosello-Diez et al., 2011). Although this approach has the disadvantage of studying a mixture of cell types rather than an isolated cell population, it allows cell properties to be explored in a more natural context, without using cell-sorting techniques that could interfere with normal cell behaviour. In this study we present the use of tissue transplantation to study epicardial cell migration and differentiation during heart regeneration in the zebrafish. Although we cannot exclude the possibility that the graft contains non-EPDC mesenchymal cells with migratory capacity, we observed that a high proportion of grafted cells express epicardial marker genes. Moreover, our analysis strongly suggests that graft-derived cells do not constitute a myocardial progenitor cell source. We also provide evidence that some cells located in the epicardial layer migrate inwards in response to injury. Grafted EPDCs have properties similar to those of endogenous EPDCs, adhering to the ventricular surface, expressing epicardial marker genes and migrating towards the injury. Interestingly, the injured myocardium displayed surface alterations that made it more adhesive to EPDCs, suggesting that increased adhesion of EPDCs to the myocardium might be important during regeneration.

We predict that the use of transgenic and mutant strains in the transplantation assay will be a valuable technique for achieving tissue-specific gain and loss of function to study mechanisms controlling epicardial EMT, migration and cell fate specification. Key signalling molecules that have been directly linked to EMT and migration during zebrafish heart regeneration include FGFs and PDGFs (Kim et al., 2010; Lepilina et al., 2006). However, both these studies lacked the EPDC-specific loss or gain of function assays that could be accomplished with the experimental setup presented here. In addition, the use of lines with ubiquitous and stable GFP expression has allowed the unbiased labelling and long-term tracking of all EPDCs.

EPDCs differentiate into myofibroblasts and perivascular fibroblasts during zebrafish regeneration

Although classically considered to be a uniform epithelial layer covering the myocardium, the epicardium is increasingly seen as a heterogeneous cell population. Genetic fate mapping of the embryonic epicardium using different epicardial Cre lines (*Wt1*, *Tbx18*, *Gata5*, *Tcf21*, *Scx* and *Sem3D*-lines) yielded incompletely overlapping results, supporting the notion that these lines do not label the entire epicardial population and might additionally label non-epicardial populations (Acharya et al., 2011; Cai et al., 2008; Chong et al., 2011; Smart et al., 2010; Zhou et al., 2011a, 2008). It is also unclear whether the adult epicardium retains characteristics of the embryonic epicardium or if it reactivates them in certain situations such as injury. During mouse development, *Wt1*$^+$ cells give rise to fibroblasts, smooth muscle cells and cardiomyocytes, but during repair in the adult they contribute primarily to myofibroblasts (Zhou et al., 2011a), suggesting that EPDCs do not have the same differentiation potential in the adult as during development.

In order to study the myocardial differentiation capacity of all epicardial cells during regeneration, we used a ubiquitous reporter line to trace EPDCs independently of their gene expression profile. Our results suggest that the zebrafish epicardium does not constitute a pool of progenitor cells for the production of new myocardium. These results support previous findings which

suggested that tcf21+ EPDCs do not differentiate into cardiomyocytes during zebrafish heart regeneration (Kikuchi et al., 2011a), and accord with lineage tracing analysis indicating that regenerating zebrafish myocardium derives from preexisting cardiomyocytes (Jopling et al., 2010; Kikuchi et al., 2010). It is important to note that EPDCs did not differentiate into cardiomyocytes even in irradiated animals, in which myocardial proliferation is impaired and regeneration might thus be expected to require an external source of progenitors. In the mouse, recent findings suggest that adult EPDCs can give rise to cardiomyocytes after in vitro culture (Chong et al., 2011) or in response to thymosin β4 stimulation in an MI-model (Smart et al., 2011). Although the contribution to regenerating myocardium in this model was modest, this finding highlights the plasticity of adult epicardium. It will be important to elucidate whether this response is conserved in zebrafish EPDCs and to study whether sensitivity to thymosin β4 exposure is similar to or greater than that described in the mouse. Epicardial cells expressing *Scleraxis* (*Scx*) and *Semaphorin* 3d (*Sema3D*) were recently shown to give rise to the coronary endothelium during development, reconciling epicardial lineage tracing studies in the mouse with the results of quail-chick proepicardial transplantations, which show a contribution of epicardium to the coronary vessel endothelium (Katz et al., 2012). It is not known whether these populations can also contribute to newly-formed vessels during regeneration. It will be interesting to study the expression and linage of Scx^+ and $Sema3D^+$ cells during zebrafish heart development and regeneration. However, our graft experiments would suggest that epicardial cells are not the main source of coronary vascular endothelial cells, since we observed little contribution of grafted *fli1a*:GFP^+ cells to host coronary vasculature. We and others previously described the accumulation of fibroblasts and myofibroblasts in the zebrafish ventricle upon cryoinjury (Chablais et al., 2011; González-Rosa et al., 2011). Our current results suggest that these cells might derive, at least in part, from the epicardium. In addition, the transplantation studies and the presence of *wt1b*:GFP^+ fibroblast-like cells surrounding coronary vessels at late post-injury stages strongly suggests that EPDCs give rise to perivascular cells. Little is known about cardiac fibroblasts in the zebrafish, and whether $tcf21^+$ and $wt1b^+$ cells label the same fibroblast population is uncertain. Fibroblast-like cells are heterogeneous and many types of fibroblast-like cells coexist in the mammalian heart (e.g., intracardiac fibroblasts, pericytes, and fibroblasts of the valves and annulus fibrosus). It thus seems likely that different EPDCs subsets give rise to different fibroblast subtypes during zebrafish heart regeneration; however, good markers distinguishing the different cardiac fibroblast-like populations are not available, and further research is required to confirm this hypothesis.

The periostin-expressing fibroblasts derived from EPDCs might serve as a cellular scaffold for regenerating cardiomyocytes and promote their proliferation. Our data additionally suggest that the epicardium supports neoangiogenesis by secreting cxcl12a and contributing perivascular fibroblasts. The mouse epicardium has also been proposed to promote neoangiogenesis through the secretion of several proangiogenic factors (Zhou et al., 2011a). Indeed, injection of human EPDCs into the mouse heart after coronary artery occlusion improves cardiac function, suggesting that EPDCs could be used therapeutically to promote post-MI recovery (Winter et al., 2007). However, the angiogenic effect provided by EPDCs in mammals is apparently insufficient to promote complete regeneration of the injured myocardium. Importantly, in the mouse, Wt1-lineage tracing after MI revealed that labelled cells remain on the heart surface (Zhou et al., 2011a). In vitro results suggest that coculture of cardiomyocytes with EPDCs enhances cardiomyocyte proliferation and promotes an efficient myofibre arrangement (Eid et al., 1992; Weeke-Klimp et al., 2010). In our experiments, wt1b:GFP cells were highly migratory. In vitro studies suggest that infiltrating EPDCs might express high levels of matrix metalloproteinases (Duan et al., 2012), and thus might contribute to the extracellular matrix remodelling necessary for cardiac regeneration. Our findings show that EPDCs invade the injured area and myocardium of cryoinjured zebrafish hearts. This closer contact established between cardiomyocytes and EPDCs might partly account for the better regenerative capacity of teleosts compared with mammals.

Acknowledgements

We thank Eduardo Díaz and others at the CNIC animal facility for zebrafish husbandry, Roisin Doohan and Ana López Aznar for tissue sections, Miguel Torres for comments on the manuscript, and Simon Bartlett for text editing. Microscopy has been carried out at the CNIC-Microscopy and Dynamic Imaging Unit. The Tg(*wt1b:eGFP*) line was provided by Christoph Englert (Fritz-Lipman Institute, Germany), the Tg(*cmlc2:nucDsRed*) line by Deborah Yelon (USCD, USA), the Tg(*cmcl2:GFP*) by Angel Raya (IBEC, Spain), the Tg(β-*actin:GFP*) line by Carl Neumann, the Tg($cmlc2:CreER^{T2}$) line by Ken Poss (Duke University, USA), the Tg(*cd41:GFP*), Tg(*ubi:loxP-GFP-loxP-mCherry*) and Tg(*fli1a:DsRedEx*) lines by Len Zon (Howard Hughes Medical Institute, USA) and the Tg(*fli1a:GFP*) and AB strains were obtained from ZIRC (Oregon, USA). MF20 and SP1.D8 antibodies were from the Developmental Studies Hybridoma Bank. We thank Darren Gilmour (EMBL, Germany), Henry Roehl (University of Sheffield, UK), Christoph Englert, José Luis Gómez-Skarmeta (CABD, Spain) and Akira Kudo (Titech, Japan) for riboprobes. Funding was from the Fundación CNIC Carlos III, the Fundación ProCNIC, the Spanish Ministry of Economy and Competiveness and the Comunidad de Madrid (FPU fellowship to J.M.G.-R., S2010/BMD-2321 FIBROTEAM fellowship to M.P., RYC-2006-001694 and BFU-2008-0012BMC to N.M.).

Appendix A. Supporting information

Supplementary data associated with this article can be found in the online version at http://dx.doi.org/10.1016/j.ydbio.2012.07.007.

References

Acharya, A., Baek, S.T., Banfi, S., Eskiocak, B., Tallquist, M.D., 2011. Efficient inducible Cre-mediated recombination in Tcf21cell lineages in the heart and kidney. Genesis.

Alexander, J.M., Bruneau, B.G., 2010. Lessons for cardiac regeneration and repair through development. Trends Mol. Med. 16, 426–434.

Ausoni, S., Sartore, S., 2009. From fish to amphibians to mammals: in search of novel strategies to optimize cardiac regeneration. J. Cell. Biol. 184, 357–364.

Cai, C.L., Martin, J.C., Sun, Y., Cui, L., Wang, L., Ouyang, K., Yang, L., Bu, L., Liang, X., Zhang, X., Stallcup, W.B., Denton, C.P., McCulloch, A., Chen, J., Evans, S.M., 2008. A myocardial lineage derives from Tbx18 epicardial cells. Nature 454, 104–108.

Carmona, R., Guadix, J.A., Cano, E., Ruiz-Villalba, A., Portillo-Sanchez, V., Perez-Pomares, J.M., Munoz-Chapuli, R., 2010. The embryonic epicardium: an essential element of cardiac development. J. Cell. Mol. Med. 14, 2066–2072.

Chablais, F., Veit, J., Rainer, G., Jazwinska, A., 2011. The zebrafish heart regenerates after cryoinjury-induced myocardial infarction. BMC Dev. Biol. 11, 21.

Chong, J.J., Chandrakanthan, V., Xaymardan, M., Asli, N.S., Li, J., Ahmed, I., Heffernan, C., Menon, M.K., Scarlett, C.J., Rashidianfar, A., Biben, C., Zoellner, H., Colvin, E.K., Pimanda, J.E., Biankin, A.V., Zhou, B., Pu, W.T., Prall, O.W., Harvey, R.P., 2011. Adult cardiac-resident MSC-like stem cells with a proepicardial origin. Cell Stem Cell 9, 527–540.

Christoffels, V.M., Grieskamp, T., Norden, J., Mommersteeg, M.T., Rudat, C., Kispert, A., 2009. Tbx18 and the fate of epicardial progenitors. Nature 458, E8-9; Discussion E9-10.

Covassin, L.D., Siekmann, A.F., Kacergis, M.C., Laver, E., Moore, J.C., Villefranc, J.A., Weinstein, B.M., Lawson, N.D., 2009. A genetic screen for vascular mutants in

zebrafish reveals dynamic roles for Vegf/Plcg1 signaling during artery development. Dev. Biol. 329, 212–226.
Duan, J., Gherghe, C., Liu, D., Hamlett, E., Srikantha, L., Rodgers, L., Regan, J.N., Rojas, M., Willis, M., Leask, A., Majesky, M., Deb, A., 2012. Wnt1/betacatenin injury response activates the epicardium and cardiac fibroblasts to promote cardiac repair. EMBO J. 31, 429–442.
Eid, H., Larson, D.M., Springhorn, J.P., Attawia, M.A., Nayak, R.C., Smith, T.W., Kelly, R.A., 1992. Role of epicardial mesothelial cells in the modification of phenotype and function of adult rat ventricular myocytes in primary coculture. Circ. Res. 71, 40–50.
González-Rosa, J.M., Martin, V., Peralta, M., Torres, M., Mercader, N., 2011. Extensive scar formation and regression during heart regeneration after cryoinjury in zebrafish. Development 138, 1663–1674.
González-Rosa, J.M., Mercader, N., 2012. Cryoinjury as a myocardial infarction model for the study of cardiac regeneration in the zebrafish. Nat. Protoc 7, 782–788.
Haas, P., Gilmour, D., 2006. Chemokine signaling mediates self-organizing tissue migration in the zebrafish lateral line. Dev. Cell. 10, 673–680.
Hendzel, M.J., Wei, Y., Mancini, M.A., Van Hooser, A., Ranalli, T., Brinkley, B.R., Bazett-Jones, D.P., Allis, C.D., 1997. Mitosis-specific phosphorylation of histone H3 initiates primarily within pericentromeric heterochromatin during G2 and spreads in an ordered fashion coincident with mitotic chromosome condensation. Chromosoma 106, 348–360.
Hidai, H., Bardales, R., Goodwin, R., Quertermous, T., Quertermous, E.E., 1998. Cloning of capsulin, a basic helix-loop-helix factor expressed in progenitor cells of the pericardium and the coronary arteries. Mech. Dev. 73, 33–43.
Higashijima, S., Okamoto, H., Ueno, N., Hotta, Y., Eguchi, G., 1997. High-frequency generation of transgenic zebrafish which reliably express GFP in whole muscles or the whole body by using promoters of zebrafish origin. Dev. Biol. 192, 289–299.
Jopling, C., Sleep, E., Raya, M., Marti, M., Raya, A., Belmonte, J.C., 2010. Zebrafish heart regeneration occurs by cardiomyocyte dedifferentiation and proliferation. Nature 464, 606–609.
Katz, T.C., Singh, M.K., Degenhardt, K., Rivera-Feliciano, J., Johnson, R.L., Epstein, J.A., Tabin, C.J., 2012. Distinct compartments of the proepicardial organ give rise to coronary vascular endothelial cells. Dev. Cell. 22, 639–650.
Kikuchi, K., Gupta, V., Wang, J., Holdway, J.E., Wills, A.A., Fang, Y., Poss, K.D., 2011a. tcf21+ Epicardial Cells Adopt Non-Myocardial Fates During Zebrafish Heart Development And Regeneration. Development.
Kikuchi, K., Holdway, J.E., Major, R.J., Blum, N., Dahn, R.D., Begemann, G., Poss, K.D., 2011b. Retinoic acid production by endocardium and epicardium is an injury response essential for zebrafish heart regeneration. Dev. Cell. 20, 397–404.
Kikuchi, K., Holdway, J.E., Werdich, A.A., Anderson, R.M., Fang, Y., Egnaczyk, G.F., Evans, T., Macrae, C.A., Stainier, D.Y., Poss, K.D., 2010. Primary contribution to zebrafish heart regeneration by gata4(+) cardiomyocytes. Nature 464, 601–605.
Kim, J., Wu, Q., Zhang, Y., Wiens, K.M., Huang, Y., Rubin, N., Shimada, H., Handin, R.I., Chao, M.Y., Tuan, T.L., Starnes, V.A., Lien, C.L., 2010. PDGF signaling is required for epicardial function and blood vessel formation in regenerating zebrafish hearts. PNAS 107, 17206–17210.
Kragl, M., Knapp, D., Nacu, E., Khattak, S., Maden, M., Epperlein, H.H., Tanaka, E.M., 2009. Cells keep a memory of their tissue origin during axolotl limb regeneration. Nature 460, 60–65.
Kreidberg, J.A., Sariola, H., Loring, J.M., Maeda, M., Pelletier, J., Housman, D., Jaenisch, R., 1993. WT-1 is required for early kidney development. Cell 74, 679–691.
Kudo, H., Amizuka, N., Araki, K., Inohaya, K., Kudo, A., 2004. Zebrafish periostin is required for the adhesion of muscle fiber bundles to the myoseptum and for the differentiation of muscle fibers. Dev. Biol. 267, 473–487.
Kuhn, B., del Monte, F., Hajjar, R.J., Chang, Y.S., Lebeche, D., Arab, S., Keating, M.T., 2007. Periostin induces proliferation of differentiated cardiomyocytes and promotes cardiac repair. Nat. Med. 13, 962–969.
Langenau, D.M., Traver, D., Ferrando, A.A., Kutok, J.L., Aster, J.C., Kanki, J.P., Lin, S., Prochownik, E., Trede, N.S., Zon, L.I., Look, A.T., 2003. Myc-induced T cell leukemia in transgenic zebrafish. Science 299, 887–890.
Lawson, N.D., Weinstein, B.M., 2002. In vivo imaging of embryonic vascular development using transgenic zebrafish. Dev. Biol. 248, 307–318.
Lepilina, A., Coon, A.N., Kikuchi, K., Holdway, J.E., Roberts, R.W., Burns, C.G., Poss, K.D., 2006. A dynamic epicardial injury response supports progenitor cell activity during zebrafish heart regeneration. Cell 127, 607–619.
Li, N., Felber, K., Elks, P., Croucher, P., Roehl, H.H., 2009. Tracking gene expression during zebrafish osteoblast differentiation. Dev. Dyn. 238, 459–466.
Limana, F., Bertolami, C., Mangoni, A., Di Carlo, A., Avitabile, D., Mocini, D., Iannelli, P., De Mori, R., Marchetti, C., Pozzoli, O., Gentili, C., Zacheo, A., Germani, A., Capogrossi, M.C., 2009. Myocardial infarction induces embryonic reprogramming of epicardial c-kit(+) cells: Role of the pericardial fluid. J. Mol. Cell. Cardiol.
Limana, F., Zacheo, A., Mocini, D., Mangoni, A., Borsellino, G., Diamantini, A., De Mori, R., Battistini, L., Vigna, E., Santini, M., Loiaconi, V., Pompilio, G., Germani, A., Capogrossi, M.C., 2007. Identification of myocardial and vascular precursor cells in human and mouse epicardium. Circ. Res. 101, 1255–1265.
Lin, H.F., Traver, D., Zhu, H., Dooley, K., Paw, B.H., Zon, L.I., Handin, R.I., 2005. Analysis of thrombocyte development in CD41-GFP transgenic zebrafish. Blood 106, 3803–3810.
Lu, J., Richardson, J.A., Olson, E.N., 1998. Capsulin: a novel bHLH transcription factor expressed in epicardial progenitors and mesenchyme of visceral organs. Mech. Dev. 73, 23–32.
Mably, J.D., Mohideen, M.A., Burns, C.G., Chen, J.N., Fishman, M.C., 2003. Heart of glass regulates the concentric growth of the heart in zebrafish. Curr. Biol. 13, 2138–2147.
Mallo, M., Schrewe, H., Martin, J.F., Olson, E.N., Ohnemus, S., 2000. Assembling a functional tympanic membrane: signals from the external acoustic meatus coordinate development of the malleal manubrium. Development 127, 4127–4136.
Manner, J., 1999. Does the subepicardial mesenchyme contribute myocardioblasts to the myocardium of the chick embryo heart? A quail-chick chimera study tracing the fate of the epicardial primordium. Anat. Rec. 255, 212–226.
Martinez-Estrada, O.M., Lettice, L.A., Essafi, A., Guadix, J.A., Slight, J., Velecela, V., Hall, E., Reichmann, J., Devenney, P.S., Hohenstein, P., Hosen, N., Hill, R.E., Munoz-Chapuli, R., Hastie, N.D., 2010. Wt1 is required for cardiovascular progenitor cell formation through transcriptional control of Snail and E-cadherin. Nat. Genet. 42, 89–93.
Mercola, M., Ruiz-Lozano, P., Schneider, M.D., 2011. Cardiac muscle regeneration: lessons from development. Genes Dev. 25, 299–309.
Moore, A.W., McInnes, L., Kreidberg, J., Hastie, N.D., Schedl, A., 1999. YAC complementation shows a requirement for Wt1 in the development of epicardium, adrenal gland and throughout nephrogenesis. Development 126, 1845–1857.
Mosimann, C., Kaufman, C.K., Li, P., Pugach, E.K., Tamplin, O.J., Zon, L.I., 2011. Ubiquitous transgene expression and Cre-based recombination driven by the ubiquitin promoter in zebrafish. Development 138, 169–177.
Perez-Pomares, J.M., de la Pompa, J.L., 2011. Signaling during epicardium and coronary vessel development. Circ. Res. 109, 1429–1442.
Perner, B., Englert, C., Bollig, F., 2007. The Wilms tumor genes wt1a and wt1b control different steps during formation of the zebrafish pronephros. Dev. Biol. 309, 87–96.
Poon, K.L., Liebling, M., Kondrychyn, I., Garcia-Lecea, M., Korzh, V., 2010. Zebrafish cardiac enhancer trap lines: new tools for in vivo studies of cardiovascular development and disease. Dev. Dyn. 239, 914–926.
Quaggin, S.E., Schwartz, L., Cui, S., Igarashi, P., Deimling, J., Post, M., Rossant, J., 1999. The basic-helix-loop-helix protein pod1 is critically important for kidney and lung organogenesis. Development 126, 5771–5783.
Robb, L., Mifsud, L., Hartley, L., Biben, C., Copeland, N.G., Gilbert, D.J., Jenkins, N.A., Harvey, R.P., 1998. Epicardin: a novel basic helix-loop-helix transcription factor gene expressed in epicardium, branchial arch myoblasts, and mesenchyme of developing lung, gut, kidney, and gonads. Dev. Dyn. 213, 105–113.
Ros, M.A., Simandl, B.K., Clark, A.W., Fallon, J.F., 2000. Methods for manipulating the chick limb bud to study gene expression, tissue interactions, and patterning. Methods Mol. Biol. 137, 245–266.
Rosello-Diez, A., Ros, M.A., Torres, M., 2011. Diffusible signals, not autonomous mechanisms, determine the main proximodistal limb subdivision. Science 332, 1086–1088.
Schnabel, K., Wu, C.C., Kurth, T., Weidinger, G., 2011. Regeneration of cryoinjury induced necrotic heart lesions in zebrafish is associated with epicardial activation and cardiomyocyte proliferation. PLoS One 6, e18503.
Smart, N., Bollini, S., Dube, K.N., Vieira, J.M., Zhou, B., Davidson, S., Yellon, D., Riegler, J., Price, A.N., Lythgoe, M.F., Pu, W.T., Riley, P.R., 2011. De novo cardiomyocytes from within the activated adult heart after injury. Nature.
Smart, N., Risebro, C.A., Clark, J.E., Ehler, E., Miquerol, L., Rossdeutsch, A., Marber, M.S., Riley, P.R., 2010. Thymosin beta4 facilitates epicardial neovascularization of the injured adult heart. Ann. N.Y. Acad. Sci. 1194, 97–104.
Sucov, H.M., Gu, Y., Thomas, S., Li, P., Pashmforoush, M., 2009. Epicardial control of myocardial proliferation and morphogenesis. Pediatr. Cardiol. 30, 617–625.
Takahashi, M., 2010. Role of the SDF-1/CXCR4 system in myocardial infarction. Circ. J.: Off. J. Jpn. Circ. Soc. 74, 418–423.
Traver, D., Paw, B.H., Poss, K.D., Penberthy, W.T., Lin, S., Zon, L.I., 2003. Transplantation and in vivo imaging of multilineage engraftment in zebrafish bloodless mutants. Nat. Immunol. 4, 1238–1246.
Traver, D., Winzeler, A., Stern, H.M., Mayhall, E.A., Langenau, D.M., Kutok, J.L., Look, A.T., Zon, L.I., 2004. Effects of lethal irradiation in zebrafish and rescue by hematopoietic cell transplantation. Blood 104, 1298–1305.
van Tuyn, J., Atsma, D.E., Winter, E.M., van der Velde-van Dijke, I., Pijnappels, D.A., Bax, N.A., Knaan-Shanzer, S., Gittenberger-de Groot, A.C., Poelmann, R.E., van der Laarse, A., van der Wall, E.E., Schalij, M.J., de Vries, A.A., 2007. Epicardial cells of human adults can undergo an epithelial-to-mesenchymal transition and obtain characteristics of smooth muscle cells in vitro. Stem Cells 25, 271–278.
Vieira, J.M., Riley, P.R., 2010. Epicardium-derived cells: a new source of regenerative capacity. Heart.
von Gise, A., Zhou, B., Honor, L.B., Ma, Q., Petryk, A., Pu, W.T., 2011. WT1 regulates epicardial epithelial to mesenchymal transition through beta-catenin and retinoic acid signaling pathways. Dev. Biol. 356, 421–431.
Vrancken Peeters, M.P., Mentink, M.M., Poelmann, R.E., Gittenberger-de Groot, A.C., 1995. Cytokeratins as a marker for epicardial formation in the quail embryo. Anat. Embryol. (Berlin) 191, 503–508.
Weeke-Klimp, A., Bax, N.A., Bellu, A.R., Winter, E.M., Vrolijk, J., Plantinga, J., Maas, S., Brinker, M., Mahtab, E.A., Gittenberger-de Groot, A.C., van Luyn, M.J., Harmsen, M.C., Lie-Venema, H., 2010. Epicardium-derived cells enhance proliferation, cellular maturation and alignment of cardiomyocytes. J. Mol. Cell. Cardiol. 49, 606–616.
Wendt, J., Radetzki, S., von Haefen, C., Hemmati, P.G., Guner, D., Schulze-Osthoff, K., Dorken, B., Daniel, P.T., 2006. Induction of p21CIP/WAF-1 and G2 arrest by ionizing irradiation impedes caspase-3-mediated apoptosis in human carcinoma cells. Oncogene 25, 972–980.

Winter, E.M., Grauss, R.W., Hogers, B., van Tuyn, J., van der Geest, R., Lie-Venema, H., Steijn, R.V., Maas, S., DeRuiter, M.C., deVries, A.A., Steendijk, P., Doevendans, P.A., van der Laarse, A., Poelmann, R.E., Schalij, M.J., Atsma, D.E., Gittenberger-de Groot, A.C., 2007. Preservation of left ventricular function and attenuation of remodeling after transplantation of human epicardium-derived cells into the infarcted mouse heart. Circulation 116, 917–927.

Zhou, B., Honor, L.B., He, H., Ma, Q., Oh, J.H., Butterfield, C., Lin, R.Z., Melero-Martin, J.M., Dolmatova, E., Duffy, H.S., Gise, A.V., Zhou, P., Hu, Y.W., Wang, G., Zhang, B., Wang, L., Hall, J.L., Moses, M.A., McGowan, F.X., Pu, W.T., 2011a. Adult mouse epicardium modulates myocardial injury by secreting paracrine factors. J. Clin. Invest.

Zhou, B., Honor, L.B., Ma, Q., Oh, J.H., Lin, R.Z., Melero-Martin, J.M., von Gise, A., Zhou, P., Hu, T., He, L., Wu, K.H., Zhang, H., Zhang, Y., Pu, W.T., 2011b. Thymosin beta 4 treatment after myocardial infarction does not reprogram epicardial cells into cardiomyocytes. J. Mol. Cell. Cardiol.

Zhou, B., Ma, Q., Rajagopal, S., Wu, S.M., Domian, I., Rivera-Feliciano, J., Jiang, D., von Gise, A., Ikeda, S., Chien, K.R., Pu, W.T., 2008. Epicardial progenitors contribute to the cardiomyocyte lineage in the developing heart. Nature 454, 109–113.